The InfraJoint Protocol for Infrared Thermography of the Hands and Wrists in the Assessment of Inflammatory Arthropathies

Rodrigo Poubel[1], Luiz Eduardo Oliveira[1], Rodrigo Gáudio[1], Flávia Pastura[2], Aura Conci[3], Vanessa Braganholo[3], Leonardo Murta[3], Ronald Sampaio[3], Ladan Machado[3]

[1]Faculdade de Medicina, Universidade Federal Fluminense, Brazil

[2]Instituto Nacional de Tecnologia (INT/MCTI), Brazil

[3]Instituto de Computação, Universidade Federal Fluminense, Brazil

{ropoubel,luiseduardooliveira,ronaldmaymone,lschulte}@id.uff.br
rodrigogaudio@yahoo.com.br, flavia.pastura@int.gov.br
{aconci,vanessa,leomurta}@ic.uff.br

Abstract. *The diagnostic differentiation between inflammatory arthropathies and non-inflammatory musculoskeletal disorders is challenging in primary care and in resource-constrained settings, where access to ultrasonography with power Doppler, computed tomography, or magnetic resonance imaging is limited. Infrared thermography of the hands and wrists is a promising low-cost, contactless and ionizing-radiation-free modality to support this triage, but its broader clinical adoption is held back by the absence of standardized acquisition protocols. In this paper we contribute (i) the InfraJoint acquisition protocol, which combines a static phase and a dynamic cooling/rewarming phase over a controlled support, and (ii) preliminary results from an ongoing cohort of patients with rheumatoid arthritis and healthy controls, characterizing the clinical profile of the recruited population and the pattern of joint involvement.*

1. Introduction

The clinical evaluation of patients with chronic joint pain is a complex and challenging task, especially for general practitioners and for clinicians who work in settings with limited access to the laboratory and imaging tests required to investigate rare and complex conditions such as systemic autoimmune and autoinflammatory diseases [Alpay-Kanıtez et al. 2019]. Joint pain may stem from a wide spectrum of etiologies, including infectious diseases (e.g., osteomyelitis), degenerative diseases (e.g., osteoarthritis), soft-tissue disorders (e.g., tendinitis, bursitis, ligament injuries), systemic inflammatory diseases (e.g., rheumatoid arthritis, psoriatic arthritis, systemic lupus erythematosus), crystal-induced arthropathies (e.g., gout), and compressive neuropathies (e.g., carpal tunnel syndrome). Differentiating inflammatory from non-inflammatory arthropathies is the first essential step to direct further investigation and treatment [Foster et al. 2023].

The diagnostic confirmation of inflammatory arthropathies typically relies on serum biomarkers and on advanced imaging exams such as joint ultrasonography with power Doppler, computed tomography (CT scan), and magnetic resonance imaging

(MRI). In regions with limited resources and a shortage of musculoskeletal specialists, this conventional pathway is hardly feasible. As a non-invasive, ionizing-radiation-free, contactless and comparatively low-cost technique, infrared thermography has been increasingly explored as a complementary tool in rheumatology [Kow and Tan 2023, Tan and Lim 2024]. However, its broader clinical adoption is held back by two interlocking problems: the absence of standardized image acquisition protocols and the lack of validated computational models that translate thermal patterns into actionable diagnostic information.

This paper presents the InfraJoint project, whose long-term objective is to enable infrared thermography as an accessible screening modality for inflammatory arthropathies of the hands and wrists. As steps towards that objective, we make two specific contributions. First, we describe a *standardized acquisition protocol* that combines a static phase with a dynamic cooling/rewarming phase over a controlled support, designed to be reproducible across visits and across acquisition sites. Second, we report *preliminary results* from the ongoing cohort, including the clinical and demographic profile of the recruited rheumatoid arthritis (RA) patients and healthy controls, the observed pattern of joint involvement, and a first analysis of the static thermal images.

The remainder of this paper is organized as follows. Section 2 characterizes the clinical problem. Section 3 surveys related work in thermography for rheumatic diseases. Section 4 details the InfraJoint image acquisition protocol. Section 5 reports preliminary results from the ongoing cohort. Section 6 concludes and outlines the next steps.

2. Clinical Context

Musculoskeletal pain in adults can be broadly partitioned into those of *non-inflammatory* and *inflammatory* causes, a distinction that is the starting point of any rheumatological workup [Foster et al. 2023]. Non-inflammatory musculoskeletal pain encompasses conditions affecting muscles, tendons, ligaments, and adjacent structures without an underlying systemic inflammatory process. Examples include osteoarthritis, tendinitis, bursitis, carpal tunnel syndrome, and fibromyalgia [Foster et al. 2023]. Although local inflammation may occur in tendinitis or bursitis, the systemic inflammatory response that characterizes autoimmune rheumatic diseases is absent.

Inflammatory arthropathies, in contrast, are typically associated with the classic signs of inflammation (e.g., pain, erythema, warmth, swelling, and loss of function), although not all of these signs are always simultaneously present, which complicates clinical recognition [Poudel and Lappin 2023]. They include immune-mediated systemic diseases (e.g., rheumatoid arthritis, psoriatic arthritis, systemic lupus erythematosus, among others), infectious arthritides, crystal-induced arthropathies (e.g., gout and pseudogout) and paraneoplastic arthropathies. The pathophysiology varies accordingly. In immune-mediated arthritides, antigen recognition triggers the recruitment of inflammatory cells (neutrophils, lymphocytes, and macrophages) to the synovial membrane, leading to chronic synovitis, fibroblast hyperplasia and, over time, to irreversible cartilage and bone destruction (left side of Figure 1) [Miyoshi and Liu 2018]. In infectious arthritis, direct microbial invasion of the joint may rapidly progress to articular destruction unless treatment is initiated early. In crystal-induced arthropathies, intra-articular deposition of monosodium urate (right side of Figure 1) or calcium pyrophosphate trig-

Figure 1. Clinical examples of inflammatory arthropathies. Left: irreversible subluxation of metacarpophalangeal joints in a patient with rheumatoid arthritis. Right: tophaceous deposits in toes secondary to gout. Source: Personal archive of Dr. Rodrigo Poubel Vieira de Rezende.

gers a neutrophil-mediated inflammatory response. The fact that joint location is itself informative (i.e., different rheumatic diseases preferentially affect different joints) has been recognized as an additional diagnostic dimension that any computational approach should exploit [Ospelt and Frank-Bertoncelj 2017].

3. Related Work

Infrared thermography is a non-invasive imaging modality that measures the temperature of an object's surface by detecting the emitted infrared radiation [Tattersall 2016]. Its physical foundation is the Stefan–Boltzmann law, according to which all bodies emit thermal radiation proportional to the fourth power of their absolute temperature [Crepeau 2009]. Modern infrared cameras convert the captured radiation into thermal images, where each pixel encodes a temperature estimate computed from the calibrated infrared signal under assumed values of surface emissivity and reflected, atmospheric and optical temperatures.

The use of infrared thermography to evaluate joint inflammation has been explored over the past decades, with renewed interest in recent years driven by improvements in sensor technology and by the demand for accessible imaging modalities. A recent review [Kow and Tan 2023] summarizes the current state of thermal imaging in RA, noting that most studies employ thermography as a static modality. They also state that protocols incorporating a dynamic functional component (cooling and rewarming) are emerging. Automated image-analysis algorithms are also being proposed.

Several recent studies have specifically examined the wrist and hand joints in RA. Tan et al. (2020) compared thermography with ultrasonography and clinical joint assessment in 37 RA patients, reporting that swollen joints showed higher mean, maximum and minimum surface temperatures than non-swollen joints, and that the thermographic findings closely mirrored those from ultrasonography. The same group later showed that thermography at the wrist may detect subclinical synovitis when compared with ultrasonography [Tan et al. 2024] and that wrist findings consistently track ultrasound findings across patients [Tan and Lim 2024].

Another study [Gatt et al. 2019] compared the thermographic patterns of hands

and wrists in 31 patients with established RA without overt clinical inflammation against 51 healthy controls using a high-resolution camera. The authors reported palm temperature distributions that crossed those of healthy controls near 31.5 °C, with consistent fingertip-to-palm gradients and noticeable inter-group differences. More recently, Triantafyllias et al. (2024) proposed a novel high-resolution thermographic marker (the Hotspot/ROI Ratio) and compared it with the joint ultrasound in patients with inflammatory arthritides, deriving thermographic cut-off values associated with active joint inflammation.

Pauk et al. (2019) reported one of the first end-to-end pipelines for disease-activity detection in RA based on an infrared thermography sensor combined with a finger examination protocol that includes static, post-cooling, and post-rewarming states. The authors compared patients with high and moderate disease activity against healthy participants and combined demographic, clinical, laboratory, and thermography parameters in their analysis, illustrating that classic features extracted from thermal images can carry a diagnostic signal beyond the static temperature value.

Gatt et al. (2015) characterized baseline thermographic patterns of the upper and lower limbs in healthy adults, providing reference data on inter-limb symmetry, intersubject variation and the typical fingertip-to-thumb temperature gradient. Methodological recommendations for clinical acquisition of musculoskeletal thermograms are codified in the guidelines of the American Academy of Thermology (2024), which prescribe patient preparation (skin cleaning, abstinence from caffeine and nicotine, removal of jewelry, avoidance of topical products), acclimatization in a temperature-controlled environment and camera-handling practices.

On the computational side, classical and deep machine-learning techniques have been applied to a variety of medical imaging problems, as surveyed by Miranda et al. (2016) . Classical techniques (e.g., Support Vector Machines, Random Forests, k-Nearest Neighbors, Bayesian, and Naïve Bayes models) typically require discrete features extracted from the image by a pre-processing stage. On the other hand, convolutional neural networks and, more recently, Transformer-based architectures, learn features directly from pixel data. Each family has trade-offs in terms of dataset size requirements, computational budget, and interpretability.

The cited literature converges on three observations that frame the InfraJoint contribution. First, methodological heterogeneity across studies (i.e., camera, distance, background, acclimatization time, occurrence of dynamic phase, and segmentation strategy) makes direct comparison and meta-analysis difficult. Second, most published work focuses on a single disease (overwhelmingly RA) and on a binary task (RA vs. healthy), rather than on the broader differential diagnosis that primary-care clinicians actually face. Third, the integration between dynamic thermal protocols and modern machine-learning pipelines is still nascent. The InfraJoint protocol described next is designed with these three gaps in mind.

4. Image Acquisition Protocol

The InfraJoint project's protocol was designed by iteratively combining the recommendations of the American Academy of Thermology (2024) with practices reported in the rheumatology literature [Kow and Tan 2023, Gatt et al. 2019, Pauk et al. 2019,

Gatt et al. 2015]. It targets the hands and wrists, regions with high prevalence of involvement in immune-mediated rheumatic diseases. The protocol is organized in five stages: (S1) environment preparation, (S2) volunteer acclimatization and clinical data collection, (S3) camera configuration, (S4) static-phase capture, and (S5) dynamic-phase capture.

S1. Environment Preparation. The acquisition room is windowless and free of air drafts. Air temperature is controlled between 20 °C and 24 °C, and relative humidity is kept between 10% and 50%. Lighting is uniform and the camera is centered between two ceiling-mounted lamps. The thermal camera (HIKMICRO SP60H L25, 640×480 pixels, thermal sensitivity below 30 mK at 30 °C) is mounted on a tripod, vertically oriented, at approximately 100 cm and at 90° from the support surface. The hands and forearms of the volunteer are placed on a 5 mm-thick, 463×395 mm Ethylene Vinyl Acetate (EVA) plate centered on a table at equal distance from both lamps. Two USB desk fans (255 mm diameter, 5 V, 7.5 W) sit on the table in front of the EVA plate, oriented towards the volunteer's hands; they are activated only during the dynamic phase. Figure 2 shows a picture of the acquisition environment.

S2. Volunteer Acclimatization and Clinical Data Collection. Before image acquisition, the volunteer remains seated in the acclimatized room for approximately 20 minutes with hands uncovered. During this period, a rheumatologist applies a structured questionnaire to collect general data (sex, date of birth, place of birth, ethnicity, and education) and health-related data (smoking, comorbidities, medications, hormone replacement, recent fever or infection, skin lesions, and pain or trauma in the hands or wrists). Information about caffeine intake, recent use of creams, lotions or sunscreen, and the presence of artificial, painted nails, or hand tattoos is also recorded. The volunteer's body temperature is measured with a clinical thermometer. Additionally, the Health Assessment Questionnaire Disability Index (HAQ-DI) is administered to patients with rheumatic diseases.

The volunteer is assigned to one of three groups: **Group A** (inflammatory arthropathy of hands and/or wrists), **Group B** (non-inflammatory pain of hands and/or wrists), or **Group C** (control). For Groups A and B, a complementary questionnaire after the imaging session records the predominant underlying pathology (rheumatoid arthritis, psoriatic arthritis, lupus, scleroderma, myopathy, gout, osteoarthritis, tendinitis/tenosynovitis, carpal tunnel syndrome, fibromyalgia, etc.), the year of diagnosis, immunological markers, and laboratory test results. The rheumatologist then performs a clinical exam by palpation and registers altered joints in a dedicated diagram (Figure 3). The patient global assessment (PGA) and the physician global assessment (PhGA) of disease activity are also registered on numerical rating scales. With this information, the Clinical Disease Activity Index (CDAI) is then calculated.

S3. Camera Configuration. A thermo-hygrometer measures the room temperature and relative humidity. These values are entered into the camera as the reflected temperature, ambient temperature, external optical temperature, and relative humidity parameters. The skin emissivity parameter is set to 0.98, as this value is widely accepted for human skin, and the focus mode is set to automatic, as it provided superior and more consistent image sharpness with minimal operator intervention in preliminary tests compared with laser and continuous modes. Two square markers (12 mm side, 5 mm height) are placed on the

Figure 2. Acquisition environment: thermal camera mounted on tripod, EVA plate (blue) on the table, USB fans positioned in front of the plate, and a white background curtain to homogenize the optical environment. The volunteer is seated facing the table during the exam.

forearms, 40 mm proximal to the dorsal flexion crease of the wrists, to provide a known scale reference within the thermographic image. The volunteer is asked to position both hands flat on the EVA plate, following a schematic drawing on the plate that defines the axes of the fingers (Figure 4). Due to the advancement of the disease, some patients may not be able to position their hands flat. We then help them position the hands and fingers as close as possible to the designated markers.

S4. Static Phase: Resting Temperature. With the hands in position, the operator touches the camera screen to trigger the autofocus, confirmed by a green rectangle overlaid on the live image. The operator then taps the camera icon to capture a single thermal image. A thumbnail of the captured image is shown to confirm the action. The static phase records the resting surface temperature distribution.

S5. Dynamic Phase: Cooling and Rewarming. With the hands still on the EVA plate, both fans are switched on at maximum speed for 2 minutes (timed with a stopwatch).

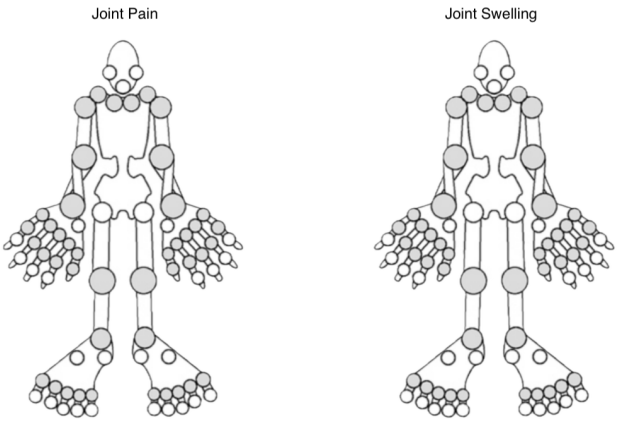

Figure 3. Joint diagram used by the rheumatologist to record altered joints, separately for joint pain (left) and joint swelling (right).

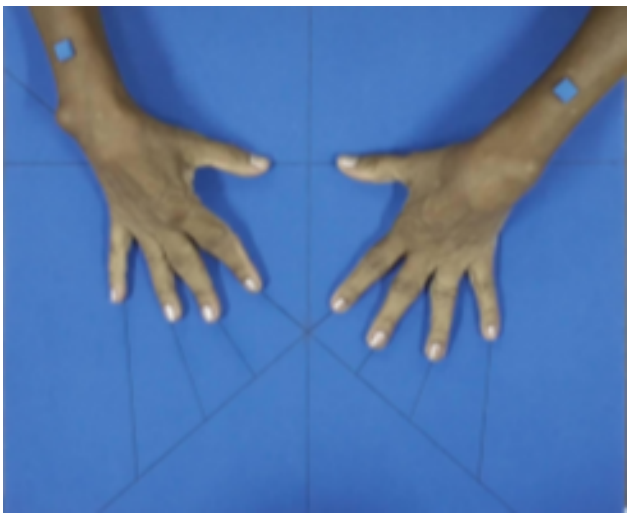

Figure 4. Hand positioning on the EVA plate following the axes defined by the schematic drawing. The square scale markers are visible on each forearm.

During this cooling interval, the operator switches the camera capture mode from single-shot to scheduled capture, configured to take 20 images at 15-second intervals (4 images per minute, totaling 5 minutes of dynamic capture). At the end of the cooling phase the fans are switched off, the operator triggers the autofocus and the scheduled capture, and the camera records the rewarming sequence. A counter (1/20) and a 15-second clock are displayed on the screen, with a notification at the end of the sequence. After the dynamic phase the camera is switched back to single-shot mode in preparation for the next volunteer.

The dynamic phase is a deliberate methodological choice. The rationale is that local inflammation alters not only baseline skin temperature but also the dynamics of vasoconstriction and vasodilation under a controlled thermal stress, so the rewarming curve provides additional, time-resolved features that may discriminate inflammatory from non-inflammatory tissue beyond what static temperatures alone reveal. This strategy is consistent with recent functional thermography work [Kow and Tan 2023, Pauk et al. 2019].

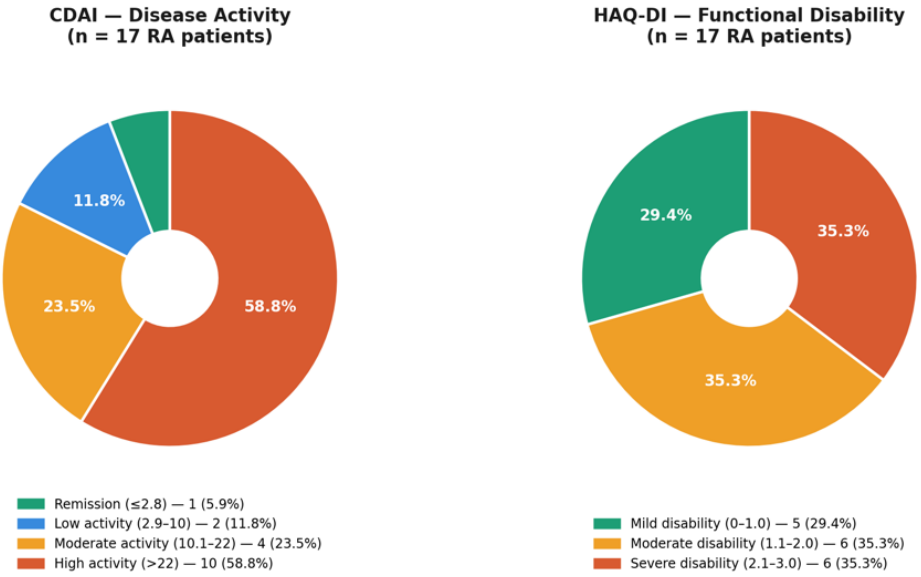

Figure 5. CDAI: Clinical Disease Activity Index (cutoffs Remission: $\leq$ 2.8; Low activity: 2.9–10.0; Moderate activity: 10.1–22.0; High activity: $>$ 22.0). HAQ-DI: Health Assessment Questionnaire - Disability Index (cutoffs: Mild disability: 0–1.0; Moderate disability: 1.1–2.0; Severe disability: 2.1–3.0). Data refer to the first evaluation timepoint (T1) of the InfraJoint project. Percentages are based on n=17 patients diagnosed with RA.

5. Preliminary Results

Recruitment began on September 23, 2025. As of April 7, 2026, we have enrolled 17 patients with RA and 15 healthy controls. The RA patients were predominantly female (94%), with mean age 59 years (SD ± 8.7) and median age 61 years (IQR: 14). Controls were predominantly male (66.6%; Fisher's exact test, $p < 0.001$) and younger, with mean age 46.7 years (SD ± 15.9) and median age 53 years (IQR: 29; Welch's t-test $p = 0.026$; Mann-Whitney U test $p = 0.034$).

Disease activity was measured using the Clinical Disease Activity Index (CDAI), a composite score based on the count of painful and swollen joints (out of 28 predefined joints), and physician and patient global assessments, independent of laboratory test values. Of 17 RA patients, 10 (58.8%) had high disease activity (CDAI $>$ 22), 4 (23.5%) moderate activity (CDAI 10.1–22), 2 (11.8%) low activity (CDAI 2.9–10), and 1 (5.9%) was in clinical remission (CDAI $\leq$ 2.8), as shown in Figure 5. The median CDAI was 26.5 (IQR: 23). Within the CDAI components, the median count of painful joints was 8 (IQR: 15) and swollen joints was 7 (IQR: 7). Physician and patient global assessment scores had medians of 3 (IQR: 2) and 8 (IQR: 5), respectively, on a 0–10 scale where 0 represents no disease activity and 10 represents maximum activity. This divergence likely reflects the different dimensions captured by each assessment: physicians primarily weigh objective signs of inflammation, whereas patients incorporate subjective symptoms such as pain, fatigue, and functional impairment, as well as comorbid conditions, which may not be fully captured by clinical or laboratory measures.

Twenty-eight regions of interest (ROIs) were evaluated by physical examination by an experienced rheumatologist. The wrists were the most frequently affected regions

Table 1. Frequency of joint involvement (tender and/or swollen) on clinical musculoskeletal examination (28-joint count).

Joint	Frequency (n, %)
Wrist-R	15 (88.2%)
Wrist-L	14 (82.4%)
Knee-R	13 (76.5%)
Knee-L	12 (70.6%)
3-PIP-R, 2-MCP-R, 2-PIP-R	10 (58.8%)
1-MCP-L, 2-MCP-L, 3-PIP-L	9 (52.9%)
5-MCP-R, 3-MCP-R, Shoulder-L	8 (47.1%)
Elbow-L, 5-MCP-L, 3-MCP-L, 1-MCP-R, Shoulder-R, 4-MCP-L	7 (41.2%)
1-IP-R, 5-PIP-L, 5-PIP-R, 4-MCP-R, 2-PIP-L	6 (35.3%)
4-PIP-R, 1-IP-L, 4-PIP-L, Elbow-R	4 (23.5%)

R = Right; L = Left; MCP = Metacarpophalangeal;
PIP = Proximal Interphalangeal; IP = Interphalangeal Thumb

(Table 1) during the physical exam. Functional disability, measured by the Health Assessment Questionnaire—Disability Index (HAQ-DI, range 0–3), had a mean of 1.657 (SD = 0.789) and median of 1.750, indicating moderate to severe functional impairment. Only 5 patients (29.4%) exhibited mild to moderate disability (HAQ-DI 0–1.0), while 12 patients (70.6%) were classified in higher impairment categories: 6 with moderate to severe disability (1.1–2.0) and 6 with severe to very severe disability (2.1–3.0).

Beyond the clinical characterization above, we conducted an initial analysis of the thermal images acquired to date. Visual inspection of the thermograms already suggests local temperature asymmetries between homologous regions of the two hands in patients with active disease, as illustrated in Figure 6, where the wrists exhibit a clearly asymmetric heat pattern. We sought to verify whether this qualitative impression is reflected systematically across the cohort.

The clinical examination summarized in Table 1 covers 28 joints (the standard 28-joint count), but several of those joints (shoulders, elbows, knees) lie outside the field of view of the InfraJoint protocol, which acquires dorsal images of both hands and wrists positioned flat on the EVA plate. Thus, our ongoing thermal analyses consider only the 11 ROIs that are accessible in this view: both wrists, and the metacarpophalangeal (MCP) and proximal interphalangeal (PIP) joints of the four long fingers, plus the metacarpophalangeal (MCP) and interphalangeal (IP) joints of the thumb. At present, we have enrolled 17 patients with RA and 15 healthy controls, in addition to a few individuals with essentially non-inflammatory rheumatic conditions. Results will be reported in future work.

6. Conclusion and Next Steps

This paper presented two contributions of the InfraJoint project. The first is a standardized acquisition protocol for infrared thermography of the hands and wrists, combining a static phase with a dynamic cooling/rewarming phase on a controlled EVA support. This protocol was designed to be reproducible across visits and acquisition sites. The second is a set of preliminary results from the ongoing cohort, characterizing the clinical and demographic profile of the recruited rheumatoid arthritis patients and healthy controls, the

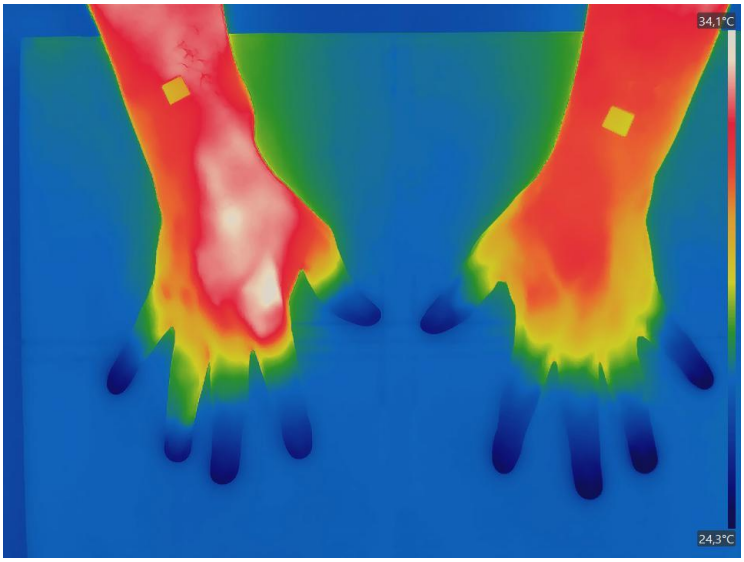

Figure 6. Thermal image of a volunteer showing visible temperature asymmetry predominantly between wrists. White regions have higher temperatures. Yellow squares on the forearms correspond to the markers we use in our protocol.

observed pattern of joint involvement, and an initial exploration of static thermal images.

The work reported here is a stepping stone towards a broader objective: enabling infrared thermography as an accessible screening tool for inflammatory arthropathies in primary care and resource-constrained settings. Several directions naturally follow from the present results. Recruitment will continue, including patients with non-inflammatory hand and wrist conditions and additional healthy controls, so that the cohort is balanced across the three groups originally defined by the protocol. We plan to make the thermal image dataset publicly available once we have a sufficient number of volunteers. On the analysis side, we plan to perform quantitative analyses of images obtained during both the static and dynamic phases of the protocol, characterizing the rewarming curves for each ROI. Moreover, we plan to evaluate machine-learning classifiers built from a richer feature set that combines per-ROI asymmetry, intra-hand gradients, and rewarming time constants. The InfraJoint project is multidisciplinary by construction, and we welcome collaboration from the rheumatology, computing, and thermal-metrology communities to refine the protocol, extend the dataset, and evaluate the resulting models in real practice settings.

Acknowledgments The authors thank the Rheumatology service of Hospital Universitário Antônio Pedro (HUAP/UFF) for access to patients and clinical infrastructure, Instituto de Computação (UFF) for providing the thermographic equipment used in this study, and the Instituto Nacional de Tecnologia (INT/MCTI) for the support in designing the acquisition environment.

Disclaimer We used the Claude Opus 4.7 model to speed up the writing of the paper. We also used Grammarly to polish grammar and language. We take full responsibility for the contents of this paper.

References

Alpay-Kanıtez, N., Celik, S., and Bes, C. (2019). Polyarthritis and its Differential Diagnosis. *European Journal of Rheumatology*, 6(4):167–173.

American Academy of Thermology (2024). Guidelines for Neuro-Musculoskeletal Infrared Medical Thermology and Sympathetic Skin Response (SSR) Studies. https://aathermology.org/organization-2/guidelines/guidelines-for-neuro-musculoskeletal-thermography/. Accessed: 2026-04-24.

Crepeau, J. (2009). A Brief History of the T4 Radiation Law. In *Proceedings of the ASME Heat Transfer Summer Conference*, pages 59–65. ASMEDC.

Foster, Z. J., Day, A. L., and Miller, J. (2023). Polyarticular Joint Pain in Adults: Evaluation and Differential Diagnosis. *American Family Physician*, 107(1):42–51.

Gatt, A., Formosa, C., Cassar, K., Camilleri, K. P., De Raffaele, C., Mizzi, A., Azzopardi, C., Mizzi, S., Falzon, O., Cristina, S., and Chockalingam, N. (2015). Thermographic Patterns of the Upper and Lower Limbs: Baseline Data. *International Journal of Vascular Medicine*, 2015(1):831369.

Gatt, A., Mercieca, C., Borg, A., Grech, A., Camilleri, L., Gatt, C., Chockalingam, N., and Formosa, C. (2019). A Comparison of Thermographic Characteristics of the Hands and Wrists of Rheumatoid Arthritis Patients and Healthy Controls. *Scientific Reports*, 9(1):17204.

Kow, J. and Tan, Y. K. (2023). An Update on Thermal Imaging in Rheumatoid Arthritis. *Joint Bone Spine*, 90(3):105496.

Miranda, E., Aryuni, M., and Irwansyah, E. (2016). A Survey of Medical Image Classification Techniques. In *2016 International Conference on Information Management and Technology (ICIMTech)*, pages 56–61. IEEE.

Miyoshi, M. and Liu, S. (2018). Collagen-Induced Arthritis Models. In *Rheumatoid Arthritis. Methods in Molecular Biology, vol. 1868*, pages 3–7. Humana Press.

Ospelt, C. and Frank-Bertoncelj, M. (2017). Why Location Matters — Site-specific Factors in Rheumatic Diseases. *Nature Reviews Rheumatology*, 13(7):433–442.

Pauk, J., Wasilewska, A., and Ihnatouski, M. (2019). Infrared Thermography Sensor for Disease Activity Detection in Rheumatoid Arthritis Patients. *Sensors*, 19(16):3444.

Poudel, P. and Lappin, S. L. (2023). Inflammatory Arthritis. StatPearls [Internet]. Treasure Island (FL): StatPearls Publishing. NBK507704. Available from: https://www.ncbi.nlm.nih.gov/books/NBK507704/.

Tan, Y. K., Hong, C., Li, H., Allen Jr, J. C., and Thumboo, J. (2020). Thermography in Rheumatoid Arthritis: A Comparison with Ultrasonography and Clinical Joint Assessment. *Clinical Radiology*, 75(12):963.e17–963.e22.

Tan, Y. K. and Lim, G. H. (2024). Assessment of Joint Inflammation at the Wrist of Patients with Rheumatoid Arthritis: Thermography Findings Closely Mirror those from Ultrasonography. *Clinical and Experimental Rheumatology*, 42(5):1051–1056.

Tan, Y. K., Lim, G. H., Ooi, C. C., Ma, V. C., and Vora, B. M. K. (2024). Thermographic and Ultrasound Assessment in Patients with Rheumatoid Arthritis: Can Thermography Detect Subclinical Synovitis at the Wrist? *BMC Rheumatology*, 8(1):62.

Tattersall, G. J. (2016). Infrared Thermography: A Non-Invasive Window into Thermal Physiology. *Comparative Biochemistry and Physiology Part A: Molecular & Integrative Physiology*, 202:78–98.

Triantafyllias, K., Clasen, M., De Blasi, M., Berres, M., Nikolodimos, E., and Schwarting, A. (2024). Performance of a Novel High-Resolution Infrared Thermography Marker in Detecting and Assessing Joint Inflammation: A Comparison with Joint Ultrasound. *Clinical and Experimental Rheumatology*, 42(9):1802–1811.